

# Comparison of Finite-Element and IEC Methods for Cable Thermal Analysis under Various Operating Environments

M. S. Baazzim, M. S. Al-Saud, M. A. El-Kady

**Abstract**—In this paper, steady-state ampacity (current carrying capacity) evaluation of underground power cable system by using analytical and numerical methods for different conditions (depth of cable, spacing between phases, soil thermal resistivity, ambient temperature, wind speed), for two system voltage level were used 132 and 380 kV. The analytical method or traditional method that was used is based on the thermal analysis method developed by Neher-McGrath and further enhanced by International Electrotechnical Commission (IEC) and published in standard IEC 60287. The numerical method that was used is finite element method and it was recourse commercial software based on finite element method.

**Keywords**—Cable ampacity, Finite element method, underground cable, thermal rating.

## I. INTRODUCTION

THE use of underground transmission and distribution cables has grown significantly over the years with the rapid increase in demand for electric energy to cover a very large expansion in populated urban areas. To meet the growing demand for electric energy, the power utilities are continuously looking for technologies to improve load handling capabilities of their underground transmission and distribution systems to use their cables to the maximum allowable ampacity rating. This leads to care of the cable temperature due to transfer of power demand and shall not exceed the specified design of cable insulation. If this temperature is exceeded, the lifetime and reliability of the cable can be reduced and it may lead to unexpected premature failure.

Two methods have been developed to calculate the cable ampacity. The first one is analytical methods or traditional methods based on the thermal analysis method developed by Neher-McGrath [1] which approximates the cable circuit configuration and assumes uniform soil conditions around the cable. Because of limited computer capability at that time, the Neher-McGrath Model has been widely accepted for over 40 years and was developed and enhanced by International Electrotechnical Commission (IEC) and published in standard IEC 60287 [2]. But such approximations and assumptions lead to inaccuracies in the calculations and often force cable engineers to use unnecessarily large safety factors and overly

conservative designs. Therefore, the analytical methods are inaccurate in ampacity computation of cables.

The second method is the numerical calculation method such as finite element method, which began to appear with the development of computers. The principle of this method is to analyze the temperature distribution in the cables and the area of the cable location. The numerical calculation method is more effective, because it considers the actual conditions, which makes the result more accurate. However, many research have been done for underground cable ampacity calculation by using finite element method for environment and condition [3]-[8] and an experiment was done to confirm that the accuracy of finite element method in steady-state ampacity [9].

In this paper, a comparison between IEC and FEM for calculating ampacity in different conditions (depth of cable, native soil thermal resistivity, ambient temperature, wind speed, spacing between phases) was done for two system voltage level 132 and 380 kV.

## II. MODEL PARAMETERS

Direct buried three-phase 132 and 380 kV cable has been modeled. Cross section of cable and parameters of cable [10] are illustrated in Fig. 1 and Table I.

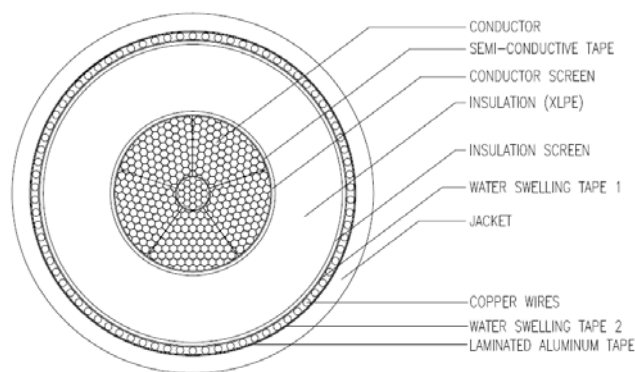


Fig. 1 Cross section cable for 132 kV and 380 kV

M.S. Baazzim is with Saudi Electricity Company, Riyadh, KSA (e-mail: msbazeem@se.com.sa).

M.S. Al-Saud and M.A. El-Kady are with the Chair in Power System Reliability and Security, College of Engineering, King Saud University, Riyadh, KSA (e-mail: mamdooh@ksu.edu.sa, melkady@ksu.edu.sa).

TABLE I  
CABLE PARAMETERS

Symbol	Parameter	Value		Units
		380 kV	132 kV	
n	Number of conductor in the cable	1	1	-
d <sub>c</sub>	Diameter of conductor	61.5	44	mm
ρ <sub>c</sub>	Thermal resistivity of copper	0.002584	0.002584	K.m/W
D <sub>semicon</sub>	Diameter over semi-conductive tape	N/A	45.2	mm
ρ <sub>semicon</sub>	Thermal resistivity of semi-conductive tape	N/A	3.5	K.m/W
D <sub>cs</sub>	Diameter over conductor screen	65.4	47.2	mm
ρ <sub>cs</sub>	Thermal resistivity of conductor screen	2.5	2.5	K.m/W
D <sub>i</sub>	Diameter over insulation	121.4	85.2	mm
ρ <sub>i</sub>	Thermal resistivity of insulation (XLPE)	3.5	3.5	K.m/W
D <sub>is</sub>	Diameter over insulation screen	125.4	87.2	mm
ρ <sub>is</sub>	Thermal resistivity of insulation screen	2.5	2.5	K.m/W
D <sub>st1</sub>	Diameter over water swelling tape 1	126.9	88.4	mm
ρ <sub>st1</sub>	Thermal resistivity of water swelling tape 1	3.5	3.5	K.m/W
D <sub>cuw</sub>	Diameter of copper wires	2.56	2.13	mm
N <sub>cuw</sub>	Number of copper wires	96	78	-
t <sub>cut</sub>	Thickness of copper tape (Open Helix)	0.13	0.15	mm
D <sub>cut</sub>	Diameter over copper tape	132	93	mm
D <sub>st2</sub>	Diameter over water swelling tape 2	134.7	93.8	mm
ρ <sub>st2</sub>	Thermal resistivity of water swelling tape 2	3.5	3.5	K.m/W
D <sub>lat</sub>	Diameter over laminated aluminum tape	135.4	94.4	mm
ρ <sub>lat</sub>	Thermal resistivity of laminated aluminum tape	0.00422	0.00422	K.m/W
D <sub>j</sub>	Diameter over jacket	144	104.4	mm
ρ <sub>j</sub>	Thermal resistivity of jacket	3.5	3.5	K.m/W

### III. IEC METHOD

IEC 60287 provides method for calculation of ampacity of cable for different design parameters of cable (cross section, thermal resistivity, thickness of layer ... etc.) as well as for different environment (ambient temperature, soil condition, depth of cable, spacing of phases ... etc.). The current rating (ampere) using in the IEC standard is

$$I = \left[ \frac{\Delta\theta - W_d [0.5 T_1 + n(T_2 + T_3 + T_4)]}{R_{ac} [T_1 + n(1 + \lambda_1)T_2 + n(1 + \lambda_1 + \lambda_2)(T_3 + T_4)]} \right]^{0.5} \quad (1)$$

where  $\Delta\theta$  [°C] is temperature rise between ambient temperature and cable conductor temperature,  $W_d$  [W/m] is dielectric loss of cable insulation,  $T_1, T_2, T_3$  [K.m/W] are equivalent thermal resistances calculated from the cable material's thermal properties,  $T_4$  [K.m/W] is the cable external thermal resistance,  $R_{ac}$  [Ω/m] is the AC electrical resistance of the cable conductor at maximum temperature and  $\lambda_1$  and  $\lambda_2$  are the ratio of losses in the metal sheath to total losses in all conductors and the ratio of losses in the armouring to total losses in all conductors, respectively.

### IV. FINITE ELEMENT METHOD

The heat transfer model developed here is for the three phase circuit. The boundary at two side of x-axis and below circuit (y-axis) are set as open boundary condition and extends to 20 m from the centre-line of the cable group [11]. The top boundary condition is set as a convective heat transfer surface. The relationship between heat flux,  $q$  [W/m<sup>2</sup>], at surface and heat transfer coefficients of convection,  $h_c$  [W/(m<sup>2</sup>.K)], are

$$q = h_c (\theta_{ground} - \theta_{air}) \quad (2)$$

where  $\theta_{ground}$  and  $\theta_{air}$  are ground and air temperature respectively, and  $h_c$  can be obtained from the following expression [11]:

$$h_c = 7.371 + 6.43v^{0.75} \quad (3)$$

where  $v$  is the air velocity in m/s.

The thermal resistivity of air gap between copper wires shall be calculated considering the radiation and convection effect and this can be derived from the following expression [12], [13]

$$\rho_{air,eff} = \frac{1}{(h_{cv} + h_r) \times d} \quad (4)$$

where  $\rho_{air,eff}$  [K.m/W] is the effective thermal resistivity of air inside the gap,  $d$  [mm] is the thickness or width of the air gap in the direction of heat flow, the  $h_{cv}$  [W/(m<sup>2</sup>.K)] and  $h_r$  [W/(m<sup>2</sup>.K)] are convective and radiative heat transfer coefficient respectively, and can be obtained by using the following expression

$$h_{cv} = \frac{Nu}{\rho_{air} \times d} \quad (5)$$

$$h_r = \frac{4\sigma T_{av}^3}{\frac{1}{\varepsilon_i} + \frac{1}{\varepsilon_o} - 2 + \frac{1}{\frac{1}{2} \left[ 1 + \left( \frac{L_h}{L_w} \right)^2 \right]^{0.5} - \frac{L_h}{L_w} + 1}} \quad (6)$$

where  $Nu$  is Nusselt number,  $\rho_{air}$  [K.m/W] is the thermal resistivity of air,  $\sigma$  [W/m<sup>2</sup>.K<sup>4</sup>] is Stefan-Boltzmann constant,  $T_{av}$  [K] is average temperature of inner and outer surface of gap,  $\varepsilon_i$  and  $\varepsilon_o$  are the emissivity of inner and outer surface respectively,  $L_h$  [mm] and  $L_w$  [mm] are the height and width of the gap.

The heat sources in cable are coming from losses in the cable and it occur in three regions of the cable; joule losses in the conductor, dielectric losses and sheath loss due to induced currents in the sheath. These losses are calculated as follows.

Joule losses: Joule loss is the heating power [W/m] of the conductor due to the resistance of the conductor and is given by

$$W_c = I^2 R_{ac} \quad (7)$$

where  $W_c$  is joule loss per unit length,  $I$  [ampere] is current, and  $R_{ac}$  is ac resistance per unit length.

Sheath Losses: Sheath loss is due to losses in the sheath or screen caused by circulating currents ( $\lambda_1'$ ) and eddy currents ( $\lambda_1''$ ) and given by

$$\lambda_1 = \lambda_1' + \lambda_1'' \quad (8)$$

In the IEC standard, sheath loss is calculated as a function of the joule loss using a multiplier,  $\lambda_1$  [2].

Dielectric Losses: Dielectric loss is due to the charge leakage and hysteresis effects in the dielectric. These can be expressed as

$$W_d = \omega C_d U_o^2 \tan \delta \quad (9)$$

where  $W_d$  [W/m] is dielectric loss of cable insulation,  $\omega = 2\pi f$  where  $f$  is the system frequency,  $U_o$  [V] is the voltage to earth,  $\tan \delta$  is the loss factor of the insulation at power frequency and operating temperature and  $C_d$  [F/m] is the insulation capacitance and can be expressed as

$$C_d = \frac{\epsilon}{18 \ln \left( \frac{D_i}{D_c} \right)} 10^{-9} \quad (10)$$

where  $\epsilon$  is the relative permittivity of the insulation,  $D_i$  [mm] is the external diameter of the insulation and  $D_c$  [mm] is the diameter of conductor, including screen.

The finite element software package ANSYS [14] was used to determine the ampacity of the cable.

## V. ANALYSIS MODEL

The analyses were done for circuit with voltage level 132 kV and 380 kV for different environmental parameter (depth of cable, thermal resistivity of backfilling and native soil, ambient temperature, wind speed and spacing between cable phases) and then calculate the steady state ampacity at maximum operating temperature of cable by using IEC method and FEM as shown in the following:

### A. Depth of Cable

The ampacity was calculated using the IEC and FEM at nine burial depths in mm for each voltage level; 100, 300, 600, 900, 1200, 1500, 1800, 2100, and 2400. The ambient temperature, wind speed, spacing between cable phases for 132 kV and 380 kV, thermal resistivity of native soil was kept 35°C, 0 m/s, 400 mm, 800 mm and 2 K.m/W respectively. Fig. 2 shows the result of ampacity versus the depth of cable.

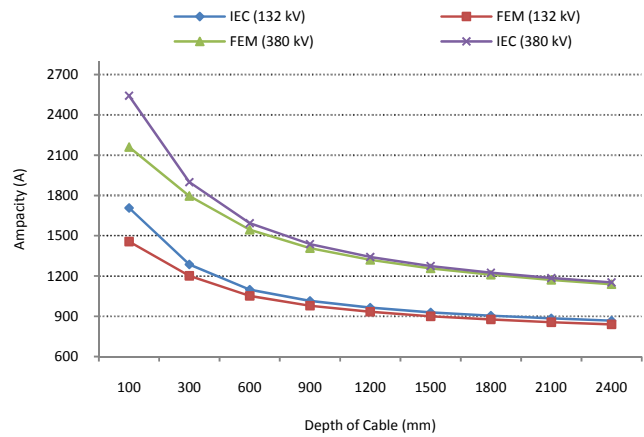


Fig. 2 Ampacity versus depth of cable

In Fig. 2 the IEC and FEM are in agreement and accurate with increasing the depth of cable unlike reducing the depth of cable.

### B. Thermal Resistivity of Soil

The twelve different thermal resistivity native soil was used to calculate the ampacity by using the IEC and FEM for each voltage level; 0.8, 1, 1.2, 1.4, 1.6, 1.8, 2, 2.2, 2.4, 2.6, 2.8 and 3 K.m/W. The ambient temperature, wind speed, spacing between cable phases 132 kV and 380 kV, depth of cable 132 kV and 380 kV was kept 35°C, 0 m/s, 400 mm, 800 mm, 1500 mm and 1700 mm, respectively. Fig. 3 shows the result of ampacity versus the thermal resistivity native soil.

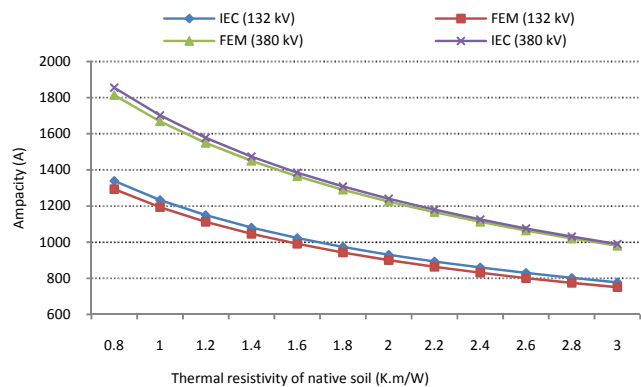


Fig. 3 Ampacity versus thermal resistivity native soil

IEC and FEM are in agreement for different thermal resistivity as show in Fig. 3. However, IEC is more accurate for 380 kV system than 132 kV because of the increasing depth of cable.

### C. Ambient Temperature

The ampacity was calculated with eleven different ambient temperature by using the IEC and FEM for each voltage level; 0, 5, 10, 15, 20, 25, 30, 35, 40, 45 and 50°C, the wind speed, spacing between cable phases 132 kV and 380 kV, thermal resistivity native soil, depth of cable 132 kV and 380 kV was kept 0 m/s, 400 mm, 800 mm, 2 K.m/W, 1500 mm and 1700

mm, respectively. Fig. 4 shows the result of ampacity versus the ambient temperature.

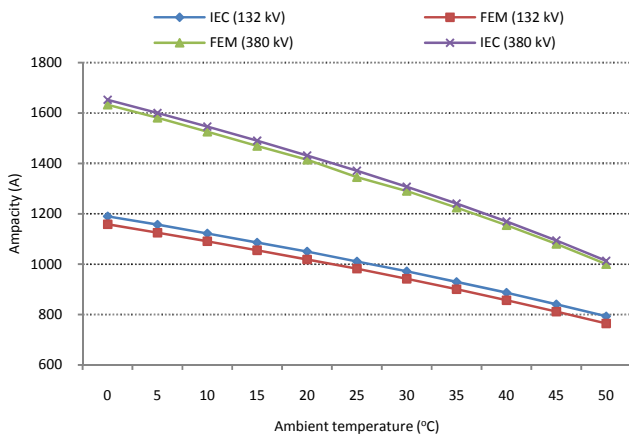


Fig. 4 Ampacity versus ambient temperature

Again the IEC and FEM are in agreement for different ambient temperature, and the accuracy of IEC for 380 kV system is more than 132 kV because the 380 kV cable is buried deeper than the 132 kV cable.

#### D. Wind Speed

The ampacity was calculated with nine different wind speed by using FEM for each voltage level; 0, 0.28, 1.389, 2.78, 5.56, 11.11, 16.67, 22.22 and 33.33 m/s, the ambient temperature, spacing between cable phases 132 kV and 380 kV, thermal resistivity native soil, depth of cable 132 kV and 380 kV was kept 35°C, 400mm, 800mm, 2 K.m/W, 1500 mm and 1700mm, respectively. Figs. 5 and 6 show the result of ampacity versus the wind speed for 132 kV and 380 kV respectively.

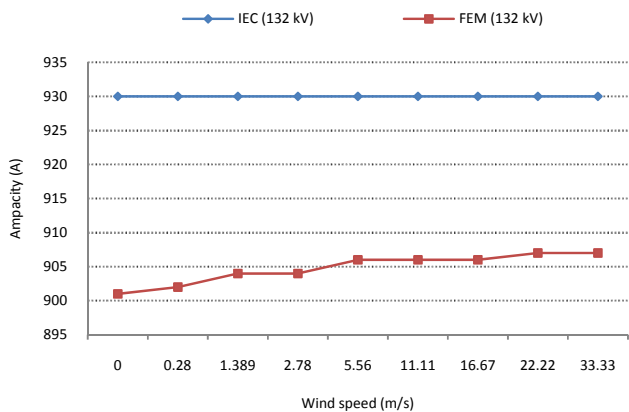


Fig. 5 Ampacity versus wind speed for 132 kV system

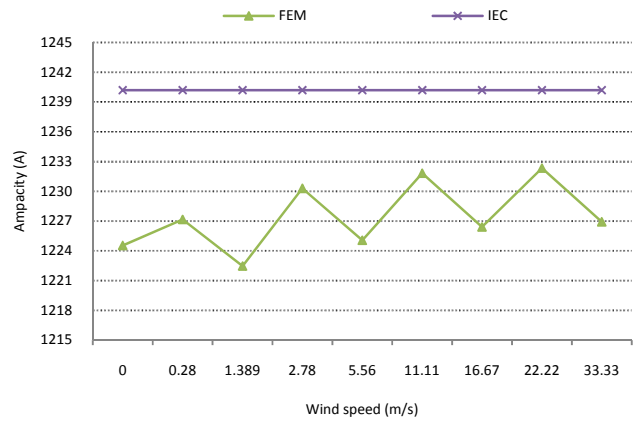


Fig. 6 Ampacity versus wind speed for 380 kV

From Figs. 5 and 6, the ampacity calculation based on IEC have no effect for changing the wind speed, while the results of FEM shows little improvement in the ampacity when increasing the wind speed. However, the wind speed has significant effect on the ampacity when reducing the depth as shown in Fig. 7, which shows the conductor temperature of middle cable (the hottest cable) versus wind speed for different depth and for both systems.

#### E. Cable Phases Spacing

The ampacity was calculated with fourteen different spacing by using IEC and FEM for 132 kV system; 150, 200, 250, 300, 350, 400, 450, 500, 550, 600, 650, 700, 750 and 800 mm, and thirteen different spacing for 380 kV system; 400, 500, 600, 700, 800, 900, 1000, 1100, 1200, 1300, 1400, 1500 and 1600 mm, the wind speed, ambient temperature, thermal resistivity of native soil, depth of cable 132 kV and 380 kV was kept 0 m/s, 35°C, 2 K.m/W, 1500 mm and 1700 mm, respectively. Figs. 8 and 9 show the result of ampacity versus the cable phases spacing for 132 kV and 380 kV respectively.

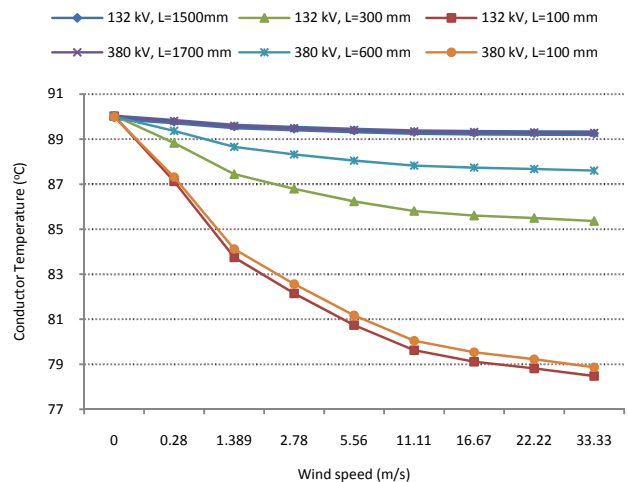


Fig. 7 Conductor temperature versus wind speed by using FEM

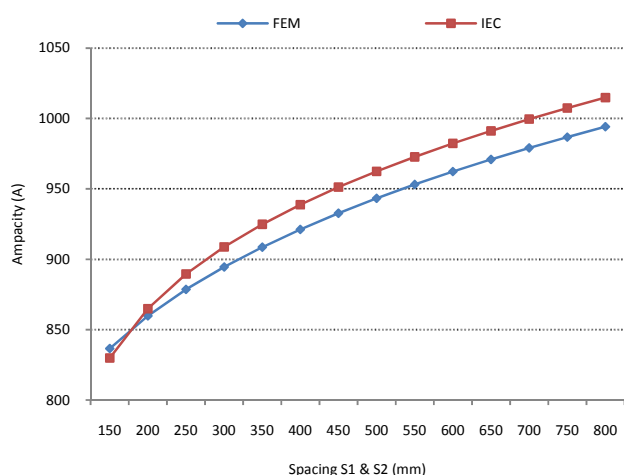


Fig. 8 Ampacity versus spacing of cable phases for 132 kV

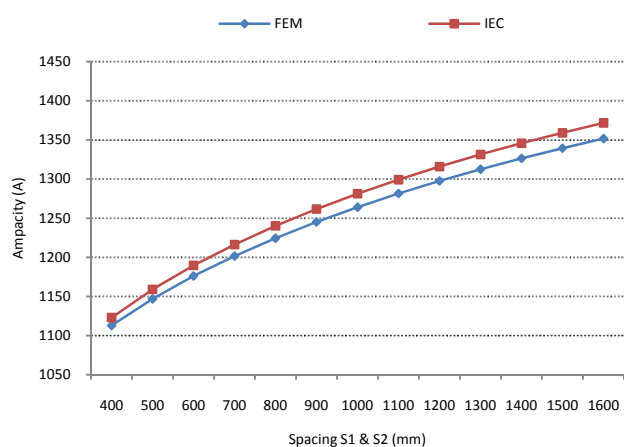


Fig. 9 Ampacity versus spacing of cable phases for 380 kV

From Figs. 8 and 9, the IEC and FEM are in agreement and IEC become more accurate when reducing the spacing between cable phases. Whenever spacing reduced, this lead to significant increase (nonlinear) loss in sheath in all cable phases due to presence of eddy current and this reduce the ampacity of cable as shown in Fig. 8 while this effect did not appear in Fig. 9 due to absence of the eddy current.

## VI. CONCLUSION

Using finite element method is more accurate and reliable in computations of underground cable ampacity as confirmed in many research. Therefore, it is used in this paper to determine the accurate of computations of underground cable ampacity by using IEC method and the conclusion are shown below:

- The IEC become more accurate with increasing the depth of cable and vice versa. In practical cases, it is recommended that the depth of the cables should be in the order of ten times their external diameter.
- IEC are in agreement with FEM for different thermal resistivity of native soil, ambient temperature and cable phases spacing.

- FEM have capability to calculate the ampacity for different wind speed unlike the IEC which does not consider it in ampacity calculation. However, the wind speed has significant effect on the ampacity when increased and the depth is reduced.

In general, the IEC method is less accurate and the results are almost higher than exact the solution and in some cases the inaccuracy is increase or limits ampacity calculations which lead to reduce reliability of using IEC in underground cable ampacity computation.

## ACKNOWLEDGMENT

This paper was supported from Saudi Electricity Company chair in power system reliability and security, King Saud University

## REFERENCES

- J. H. Neher and M.H. McGrath, "The Calculation of the Temperature Rise and Load Capability of Cable Systems", *AIEE Transactions – Power Apparatus and Systems*, Part III, Vol. 76, Issue 3, Apr. 1957, pp. 752-764.
- IEC 60287, "Calculation of the Current Rating (100% Load Factor)", 2006.
- Francisco de Leon, George J. Anders, "Effects of Backfilling on Cable Ampacity Analyzed With the Finite Element Method", *IEEE Transactions on Power Delivery* Vol. 23, No. 2, April 2008.
- Youyuan Wang, Rengang Chen, Weigen Chen, Jian Li, Lin Du, Qing Yang, "Calculation of the Current Carrying Capability of Duct Laying Electric Cable and Analysis of the Influential Factors", *2010 IEEE International Power Modulator and High Voltage Conference (IPMHVC)*, pp 735-738, Atlanta, GA, USA, 23-27 May 2010.
- M. S. Al-Saud, M. A. El-Kady, R. D. Findlay, "Accurate Assessment of Thermal Field and Ampacity of Underground Power Cables", *2006 Canadian Conference on Electrical and Computer Engineering (CCECE '06)*, pp 651-654, Ottawa, Canada, May 2006.
- M. S. Al-Saud, M. A. El-Kady, R. D. Findlay, "Advanced Thermal Field Sensitivity Analysis of Power Cables", *2007 Canadian Conference on Electrical and Computer Engineering (CCECE '07)*, pp 133-136, Vancouver, Canada, 22-26 April 2007.
- S. Kahourzade, A. Mahmoudi, B. Nim Taj, O. Palizban, "Ampacity Calculation of the Underground Power Cables in Voluntary Conditions by Finite Element Method", *2011 8th International Conference on Electrical Engineering/Electronics, Computer, Telecommunications and Information Technology (ECTI-CON)*, pp 657-660, Khon Kaen, Thailand, 17-19 May 2011.
- M. A. Mozan, M. A. El-Kady, A. A. Mazi, "Advanced Thermal Analysis of Underground Power Cables", *5th International Middle East Power Conference (MEPCON'97)*, pp 506-510, Alexandria, Egypt, 4-6 January 1997.
- M. S. Al-Saud, M. A. El-Kady, R. D. Findlay, "Combined Simulation–Experimental Approach to Power Cable Thermal Loading Assessment", *IET Generation, Transmission & Distribution*, Vol. 2, No. 1, Jan. 2008, pp. 13-21.
- From Saudi Electricity Company documents, Riyadh, 2013.
- Yongchun Liang, "Steady-state Thermal Analysis of Power Cable Systems in Ducts Using Streamline Upwind/Petrov-Galerkin Finite Element Method", *IEEE Transactions on Dielectrics and Electrical Insulation* Vol. 19, No. 1, February 2012.
- ES ISO 15099, "Thermal Performance of Windows, Doors and Shading Devices-Detailed Calculations", 2012.
- C. Hannan, "Measurements and Modeling of Air and Flow in a Brick Wall Cavity", Master thesis, Concordia University, Montreal, Quebec, Canada, 2007.
- ANSYS Finite Element Simulation Software, ANSYS Inc., Canonsburg, PA, USA.

**Mohammed S. Baazzim** Received his B.Sc. degree from King Saud University, College of Engineering, Electrical Engineering Department in 2002. Since then he has been working at Saudi Electricity Company in EHV engineering and design department. He is now enrolled in King Saud University for his M.Sc in the field of design and operation of underground cables.

**M. S. Al-Saud** Received his Ph.D. in 2007 from McMaster University, Canada. He is currently Associate Professor at the Electrical Engineering Department, King Saud University. He is also the Deputy Dean of the Advanced Manufacturing Institute at the College of Engineering, King Saud University and a Consultant at King Abdulaziz City for Science and Technology. His research areas include: design and operation of distribution system, power system reliability and security assessment, application of artificial intelligence in power system design, load management in smart grid and renewable energy.

**M. A. El-Kady** Received his Ph.D. from McMaster University, Canada in 1980. Since then, he has held a dual University/Industry career both at McMaster University and Ontario Hydro, Canada. At McMaster University, he progressed through academic ranks until he became a Professor in 1991 while teaching and supervising research in power system planning and operation. At Ontario Hydro, he progressed through several engineering and management positions where he ultimately filled the position of Development Planning Manager in 1986. He has been (since 1993) with the College of Engineering, King Saud University, Saudi Arabia. He has authored and co-authored over 300 publications in various power system and engineering topics. In addition to his academic activities, he has also been participating in industry funded projects and studies on issues relating to re-structuring of power utilities, energy market studies, development of bulk electricity plans, standardization of electricity services, energy efficiency, and environmental assessment.